The Thesis Committee for Shannon Renee Sweeney
Certifies that this is the approved version of the following thesis:

Untargeted Metabolomics Analysis of Rheumatoid Arthritis Patient Sera Before and After Rituximab Treatment

APPROVED BY
SUPERVISING COMMITTEE:

Supervisor: _____
Stefano Tiziani

Co-Supervisor: _____
Monica Guma

Untargeted Metabolomics Analysis of Rheumatoid Arthritis Patient Sera Before and After Rituximab Treatment

by

Shannon Renee Sweeney, B.A.

Thesis

Presented to the Faculty of the Graduate School of

The University of Texas at Austin

in Partial Fulfillment

of the Requirements

for the Degree of

Master of Arts

The University of Texas at Austin

August 2015

Acknowledgements

Heartfelt gratitude to Dr. Stefano Tiziani and Dr. Monica Guma for their thoughtful guidance, saintly patience, and unwavering support along this journey.

Additional thanks to the exceptional scientists who were involved in this project and without whom this work could not have been completed: Dr. Alessia Lodi, Dr. Bo Wang, Dr. Arthur Kavanaugh, and Dr. David Boyle.

Many thanks to Dr. Andrew Hinck and Dr. Kristin Cano-McCue for their technical support during data acquisition at the Biomolecular NMR facility at the University of Texas Health Science Center at San Antonio (UTHSCSA).

Abstract

Untargeted Metabolomics Analysis of Rheumatoid Arthritis Patient Sera Before and After Rituximab Treatment

Shannon Renee Sweeney, M.A.

The University of Texas at Austin, 2015

Supervisors: Stefano Tiziani, Monica Guma

Background: Rheumatoid arthritis (RA) is an autoimmune disease with no known cure that affects approximately 1.3 million Americans. RA patients suffer from chronic pain and inflammation and are faced with probable disability, reduced life expectancy, and increased risk of several other diseases. In the last decade, biological therapies have revolutionized RA treatment. Although administration of a tumor necrosis factor (TNF) neutralizing agent is the first-line biological therapy, many RA patients show only partial or no clinical response to treatment. Subsequently, anti-B cell, anti-T cell, or anti-IL6 therapies can be evaluated. Streamlining of treatment protocols is necessary to improve patient outcomes.

Methods: Serum was collected from 23 active, seropositive RA patients on concomitant methotrexate, at baseline and six months after treatment with rituximab. Based on the American College of Rheumatology improvement criteria, at a level of 20% (ACR20), patients were categorized as either responders or non-responders. An untargeted metabolomics approach was used to characterize the serum metabolome of patients. High

resolution one-dimensional ^{1}H-NMR spectra were acquired using a Bruker Avance 700 MHz spectrometer. In addition, A Thermo Scientific Q Exactive Hybrid Quadrupole-Orbitrap mass spectrometer was used for UPLC-MS/MS of serum lipids. Data processing, statistical analysis, and pathway mapping were performed in MATLAB in conjunction with several metabolomics software packages including, NMRLab, MetaboLab, Chenomx, MetaboAnalyst, MetaboSearch, VANTED, Xcalibur, and Sieve.

Results: Based on the ACR20 criteria, at baseline, 14 patients were characterized as responders and 9 patients were considered non-responders. Similarly, 20 patients followed-up at six months, 13 responders and 7 non-responders. Seven polar metabolites and 15 unique lipid species achieved a p-value of less than 0.05 for a two sample t-test prior to treatment with rituximab. Following rituximab therapy, five polar metabolites and 37 lipid species were statistically significant between groups. Pathway analysis of both polar and apolar metabolites revealed metabolic differences between responder and non-responders before and after treatment with rituximab.

Conclusion: A clear relationship between blood metabolic profiles and clinical response to rituximab therapy suggests that ^{1}H-NMR and UPLC-MS/MS are promising tools for RA therapy optimization and acceleration of treatment protocols to improve patient outcomes.

Table of Contents

List of Tables

List of Figures

I. Introduction

Rheumatoid arthritis (RA) is a common autoimmune disease that affects approximately 1.3 million Americans (1) and an estimated 0.5 - 1% of the global population (2, 3). Invasion of immune cells and characteristic chronic inflammation lead to painful cartilage and joint destruction and poor long term outcomes (3, 4). RA patients suffer from probable disability, diminished life expectancy, and increased risk of other diseases (2, 4, 5). Greater understanding of the pathogenesis of RA has transformed the therapeutic options available to people afflicted with the disease (4). Therapy for RA was revolutionized a decade or so ago by the introduction of biological agents, especially agents that target the inflammatory cytokine tumor necrosis factor (TNF) (2). Current treatment protocols typically involve sequentially evaluating biological therapy options until an acceptable level of disease control is achieved. The initial, first-line therapy involves a TNF neutralizing treatment, such as infliximab (6). However, a significant number of patients exhibit only partial or no therapeutic response to anti-TNF treatments (4, 7-9). Following anti-TNF failure, patients may be treated with anti-B cell (rituximab), anti-T cell (abatacept), or anti-IL6 (tocilizumab) therapy.

Early detection and initiation of an effective treatment are critical for minimizing damage caused by the disease, improving immediate and long-term patient outcomes, and quality of life (10). Aggressive treatment is paramount if the damage caused by RA is to be controlled (4). In particular, successful disease management requires better tools for diagnosis and streamlining of treatment protocols (9, 10). Thus, choosing and initiating the right biological treatment earlier in the course of the disease could help to reach the goal

of remission. A greater effort should be made to develop the tools necessary to employ a personalized medicine approach, in an attempt to match patients with the most appropriate therapy option for their disease subtype.

Given the complexity and heterogeneity of RA, it seems doubtful that a single cytokine or biomarker will be sufficient for therapy discrimination. Instead, biomarker signatures may represent more realistic approach to personalized therapeutic protocols for those suffering from the disease (11). Once genetic and epigenetic risk factors and environmental triggers have led from preclinical to clinical disease, RA may be driven by several different factors. These factors include cytokines such as TNF or IL-6, or different cell subset, such as B-cell, T-cell or macrophages, which ultimately lead to a perpetuating cycle of chronic synovitis (4). Identifying these unique signatures could make a significant difference in RA management and attainment of disease remission.

Variations in metabolite concentrations can also serve as diagnostic or prognostic biomarkers. We propose that the study of metabolomics in inflammatory diseases can be useful to identify biomarker signatures. Metabolomics is the science of identifying and quantifying the biochemical byproducts of cellular metabolism, frequently referred to as metabolites. The goal of metabolomics is to comprehensively measure the small molecules present in a specific cell, tissue, organ, organism, or biofluid (12, 13). Metabolomics has many applications and is frequently used to identify single biomarkers, classify metabolite patterns of health or disease, elucidate pathways involved in pathogenesis, uncover novel targets for modulation of dysregulated pathways, and to monitor treatment and/or disease status (13, 14). Recent studies in other fields, such as oncology, demonstrate the

applicability of metabolomics using serum and urine samples for diagnosis and prognosis. The application of metabolomics to the field of cancer research has demonstrated that nuclear magnetic resonance spectroscopy (NMR) and mass spectrometry (MS) can be useful tools for characterizing the metabolic dysregulation that is a signature of the complex and heterogeneous disease (15-20). Similar to cancer, RA is a complex and heterogeneous disease that requires a personalized approach to treatment. However, little is known about the metabolome in RA and how it can be used for diagnosis and treatment evaluation.

The application of metabolomics to RA is still in its infancy, but early studies have yielded promising results. One study published in 2011 found that serum metabolites detected by MS successfully distinguished metabolic profiles of individuals with RA, psoriatic arthritis (PsoA), and heathy controls and concluded that serum metabolite profiling could be a useful diagnostic tool. Specifically, they found elevated levels of glyceric acid, D-ribofuranose, and hypoxanthine, while histidine, threonic acid, methionine, cholesterol, asparagine, and threonine were lower in RA patients compared to healthy controls (21). Another study assessed synovial fluid metabolite profiles with MS and found 20 potential biomarkers for differentiating RA from other types of inflammatory arthritis. Notably, citrulline, succinate, glutamine, octadecanol, isopalmitic acid, and glycerol were identified (22). Similarly, a lipidomics analysis of synovial fluid demonstrated that lipid profiles are dependent upon both disease type (osteoarthritis (OA) or RA) and stage (early or late OA). The researchers proposed that these changes may be the result of compensatory lubrication mechanisms and/or related to inflammation and may

be disease and stage of progression specific signatures (23). These studies suggest that metabolomics analyses of several different biological fluids may be useful diagnostic tools prior to initiation of treatment and may also prove effective for earlier detection of RA. In addition, an NMR analysis of baseline urine metabolomes successfully discriminated RA patients based on their response to anti-TNF therapy. Specifically, histamine, glutamine, xanthurenic acid, and ethanolamine were detected in RA patient urine and significantly contributed to differences between response groups (9). These findings indicate that metabolic profiling has the potential to effectively predict patient response to therapy prior to administration. Here we show that an untargeted analysis of polar and lipid metabolites from serum samples by 1D ^{1}H-NMR and UPLC-MS/MS is a promising clinical tool for predicting response to rituximab therapy and ultimately improving patient outcomes.

II. Methods

Patients

The ARISE (Assessment of Rituximab's Immunomodulatory Synovial Effects registered at ClinicalTrials.Gov NCT00147966) clinical trial was recently described in detail (8). Briefly, the study enrolled persons between the ages of 18–70 years with an established diagnosis of RA and a positive serum test for rheumatoid factor (RF). Patients were required to have active disease (defined as a tender joint count ≥8/68, a swollen joint count ≥6/66, and either early morning stiffness ≥45 min in duration or an elevation in erythrocyte sedimentation rate (ESR) ≥28 mm/h or C-reactive protein (CRP) ≥1.5 mg/dl), despite the concomitant use of methotrexate (MTX) at a dose of ≥12.5 mg/week for at least 12 weeks. Concomitant use of non-steroidal anti-inflammatory drugs and oral prednisone at doses of 10 mg/day or less were permitted, provided dosing was stable for at least 4 weeks before the study. Patients previously treated with tumor necrosis factor (TNF) inhibitors were permitted to enroll in the study provided they had been off therapy for ≥2 months for etanercept and ≥3 months for adalimumab or infliximab. Exclusion criteria included prior treatment with rituximab, active or recent infections, pre-existing malignancy, and a history of infection with HIV or hepatitis B or C. Patients received 1 g rituximab intravenously on day 0, and again on day 14, in the absence of peri-infusion steroids. Blood was collected on day 0, and at 2 and 6 months following treatment. Of 23 enrolled patients, 20 patients completed the 6-month protocol and are included in the serum analysis. Local Institutional Review Board (University of California at San Diego

Institutional Review Board) approval was obtained, and all patients signed written informed consent before study entry (8).

Clinical Outcomes

The primary clinical outcome was response according to the American College of Rheumatology (ACR) improvement criteria, at a 20% level (ACR20), at 6 months (8). Secondary clinical outcomes included ACR20, as well as, ACR50 and ACR70 responses at monthly time points, Disease Activity Score using a 28 joint count (DAS28) (24), and changes in individual disease activity parameters: tender joint count, swollen joint count, physician global assessment of disease, patient global assessment of disease, patient assessment of pain, measure of functional status using the Health Assessment Questionnaire (HAQ), and CRP and ESR at monthly time points.

Metabolomics Sample Preparation

Frozen human serum samples were provided by Dr. Monica Guma from the Division of Rheumatology, Allergy, and Immunology at the University of San Diego, School of Medicine (La Jolla, CA). Samples were de-identified, shipped on dry ice, and stored at -80°C prior to analysis. Lipid and protein fractions were removed via ultrafiltration (Nanosep 3K OMEGA, Pall Corporation, Ann Arbor, MI) at 4°C (25). A 160 µL aliquot of filtered biofluid was used for NMR analysis. The biofluid was combined with 20 µL of D_2O and 20 µL of phosphate buffer containing TMSP-d4 and sodium azide (final concentrations 100 mM, 0.1 mM, and 0.05% (w/v) respectively). Samples were centrifuged

at maximum speed for 10 minutes at 4°C to remove any insoluble particulates and a 180 μL aliquot of each prepared sample was transferred to a 3 mm NMR tube (Norell, Landisville, NJ) prior to data acquisition.

The apolar metabolites were recovered from the filter with two successive washes with 250 μL of 0.9% saline (20). Samples were spiked with the following stable isotopically labeled internal standards: 1,2-dipalmitoyl-d62-sn-glycero-3-phosphoethanolamine (16:0 PE-d62), 1,2-dimyristoyl-d54-sn-glycero-2-[phospho-L-serine] sodium salt (14:0 PS-d54), 1,2-dilauroyl-sn-glycero-2-phosphocholine (12:0 PC), 1,2-dioleoyl-sn-glycero-3-phosphoinositol ammonium salt (18:1 PI), Ceramide/Sphingoid Internal Standard Mixture I (Avanti Polar Lipids Inc., Alabaster, Alabama), and heptadecanoic-17,17,17-d3 acid (CDN Isotopes, Pointe-Claire, Quebec, Canada). Recovered lipids were isolated via extraction by adding the 500 μL saline solution to 500 μL methanol and 1 mL chloroform in a glass vial. Individual samples were vortexed immediately to ensure protein denaturation. Subsequently, samples were agitated on a platform shaker (Heidolph, Elk Grove Village, IL) for 10 minutes at 2500 rpm. Phase separation was achieved by centrifugation at 4750 rpm for 20 minutes at 4°C. For each sample, 200 μL aliquot of the lipid containing chloroform phase was transferred into glass tube. Aliquots were dried at -4°C with a CentriVap Concentrator (Labconco, Kansas City, MO). Dried lipids were resuspended in 200 μL of 65:30:5 acetonitrile:isopropanol:water and transferred into glass liquid chromatography (LC) autosampler vials with 300 μL fused inserts (Supelco, Bellefonte, PA).

Nuclear Magnetic Resonance Spectroscopy Acquisition and Data Processing

A 16.4 T (700MHz) Bruker Avance spectrometer equipped with a 5 mm TCI cryogenically cooled probe and autosampler (Bruker BioSpin Corp., Billerica, MA) was used to acquire spectra. Samples were permitted to equilibrate in the magnet prior to acquisition. A one dimensional ^{1}H-NMR pulse sequence with excitation sculpting water suppression was used for data acquisition (26). Spectra were processed with NMRLab and MetaboLab (27) in the MATLAB programming environment (MathWorks Inc., Natick, MA). Metabolite concentrations were normalized to the TMSP-d4 peak. Post-processing for statistical purposes included alignment, scaling, exclusion of the regions containing the water and TMSP peaks, and generalized log transformations (28). Metabolite assignment and quantification was performed using Chenomx NMR Suite (Chenomx Inc., Edmonton, Alberta, Canada), the Birmingham Metabolite Library (29), and the Human Metabolome Database (30).

Mass Spectrometry Acquisition and Data Processing

A Q Exactive Hybrid Quadrupole-Orbitrap Mass Spectrometer equipped with an Accela 1250 pump and autosampler (Thermo Scientific, Waltham, MA) was used for UPLC-MS/MS analysis of the serum lipid fractions. Separation was achieved on a Kinetex 2.6 µm C-18 100 Å column (Phenomenex, Torrance, CA). Mobile phase A was an 80:20 solution of water and acetonitrile containing 10 mM ammonium acetate and 0.05% (w/v) formic acid. Mobile phase B was a solution of 90:9:1 isopropanol:acetonitrile:water with 10 mM ammonium acetate and 0.05% (w/v) formic acid. The chromatography gradient

began with 90% mobile phase A, decreasing to 5% mobile phase A over 20 minutes, holding at 5% mobile phase A for an additional 7 minutes, and then gradually increasing back to 90% mobile phase A over 8 minutes to re-equilibrate the column prior to injection of the subsequent sample. The total chromatography run time was 35 minutes at a flow rate of 0.3 mL/min. The UPLC system was coupled to the spectrometer with an electrospray ionization source (ESI) and spectra were recorded in both negative and positive ionization modes for maximal metabolite coverage. For negative ionization mode, the spray voltage and capillary temperature were set at 3.0 kV and 300°C, respectively. For positive ionization mode, the spray voltage was adjusted to 2.5 kV and the capillary temperature was decreased to 275°C. For both acquisition modes, the sheath and auxiliary gas flow rates were set to 45 and 11 units, respectively. Solvent blanks and pooled quality controls were injected periodically to monitor column carry over and instrument stability.

Data acquisition was performed using the Thermo Scientific software package Xcalibur and then further imported into Sieve Software 2.1 (Thermo Scientific) for processing. The features obtained in Sieve were then imported and analyzed in MATLAB. Spectra deconvolution were processed according to mass accuracy and retention time. Metabolite assignment was done at a 5 ppm mass accuracy range by interrogation of several databases including KEGG (31), LIPID MAPS (32), Human Metabolome Database (HMDB) (30), Madison Metabolomics Consortium Database (MMCD) (33), and Metlin (34), in part using MetaboSearch (35), a software tool developed for untargeted MS-based metabolomics. Intensities were normalized to internal standards that were present in all samples. For negative ionization mode, heptadecanoic-17,17,17-d3 was used. (2S,3R)-2-

aminoheptadecane-1,3-diol (Sphinganine C17) was used for normalization of intensities generated in positive ionization mode. Following normalization, metabolites identified in each mode were merged to generate a composite list of metabolites prior to statistical analysis in MATLAB. Where accurate masses and retention times were associated with multiple lipid classes, MS/MS analysis was performed to fragment the molecules of interest to improve assignment confidence.

Statistical Analysis

For individual metabolites, statistical significance was evaluated using a two-sample t-test (statistical significance: *$p<0.10$, **$p<0.05$, and ***$p<0.01$). Multivariate analysis was performed using PLS-Toolbox (Eigenvector Research, Manson, WA) in the MATLAB programming environment. Supervised partial least squares discriminant analysis (PLSDA) was used to evaluate global differences between responders and non-responders before and after treatment with rituximab. Polar metabolite correlation relationships were reported as Pearson's correlation coefficients and visualized as a heat map and hierarchical clustering analysis with Euclidean distance metric in MATLAB.

Pathway Analysis

MetaboAnalyst 3.0 (http://www.metaboanalyst.ca/) was used identify pathways of significant interest involving polar metabolites (36, 37). In addition, VANTED (http://vanted.ipk-gatersleben.de/) software was used for pathway analysis of statistically significant lipid classes (38). The upregulation or downregulation of individual lipid

species was evaluated by calculating the fold change between responders and non-responders. A global test algorithm was applied to determine the overall significance of each pathway between the two groups (39). Relative abundances are reported as colors to indicate the direction of statistically significant differences between groups. Polar and apolar pathways were manually integrated to provide a more comprehensive picture of the overall metabolic dysregulation found in rheumatoid arthritis patients relative to response to rituximab therapy.

III. Results

Patient Response to Rituximab Therapy

Following treatment, patients were categorized as either rituximab responders or non-responders as determined by ACR criteria. Patients who attained a 20% (ACR20) or greater improvement in their disease were classified as responders (8). At baseline, 14 patients were classified as responders and the remaining 9 patients were considered non-responders (**Table 1**). Similarly, of the 20 patients who follow-up at six months, 13 were in the responder group and the remaining 7 were in the non-responder group.

Metabolomics Approach to Data Collection and Analysis

An unbiased, untargeted metabolomics technique was applied to both MS and NMR experiments. Polar and apolar fractions were prepared for all 43 samples. The polar fractions were analyzed by 1D ^{1}H-NMR, while lipids were analyzed by UPLC-MS/MS. Using multiple databases, a total of 48 metabolites were identified and quantified from the NMR spectra (29, 30). Polar metabolites were predominantly amino acids, ketone bodies, and intermediates of energy metabolism. A complete list of polar metabolites, mean concentrations and standard deviations, and reference values are listed in **Table 2**. While several metabolite concentrations detected were abnormal, many were within previously measured normal ranges, indicating that a single metabolite biomarker is unlikely for RA, but a disease specific profile signature is still possible. Including internal standards, interrogation of several reference libraries yielded 584 identifiable unique lipid compounds from the apolar fraction (30-35). Several major classes of lipids were well represented

including: phosphatidic acids (PA), phosphatidylcholines (PC), phosphatidylethanolamines (PE), phosphatidylglycerols (PG), phosphatidylinositols (PI), phosphatidylserines (PS), sphingomyelins (SM), ceramides (Cer), sterols, triglycerides (TG), and free fatty acids. In addition to standard ester linkage glycerophospholipids, alkyl ether and alkenyl ether linkages were also detected, as indicated by an O- or P- prefix, respectively. Lipid species that were statistically significant between responders and non-responders before and after treatment can be found in **Table 3** and **Table 4**, respectively. Following normalization, UPLC-MS and ^{1}H-NMR data sets were scaled and combined for multivariate statistical analysis.

Differences in Metabolite Profiles Before Treatment

Polar metabolite profiles of patient sera before rituximab therapy was accomplished using 1D ^{1}H-NMR spectroscopy. Mean spectra for responders and non-responders before rituximab administration are shown in **Figure 1a**. Fitting of the ^{1}H-NMR spectra revealed 13 polar metabolites that achieved a p-value less than 0.10 when a two sample t-test was performed. Seven of these metabolites, phenylalanine, 2-hydroxyvalerate, succinate, choline, glycine, acetoacetate, and tyrosine, achieved a p-value of less than 0.05 (**Figure 2a**). Interestingly, all of the significant metabolites were lower in responders relative to non-responders. Mean spectra (**Figure 1a**) show that most, but not all, features are diminished in responders. Unexpectedly, Pearson's correlation coefficients show that the relationships between polar metabolites are all positive. Not surprisingly, metabolites primarily cluster into groups according to their biological function or chemical

classification. For example ketone bodies, branched chain amino acids, and aromatic amino acids form close associations on the heat map (**Figure 3**).

Apolar metabolites were isolated by UPLC-MS/MS in both negative and positive modes for the most complete lipidome coverage. Thousands of features were detected in the MS spectra. Of which, 584 were matched to known compounds reported in a number of established libraries. A two sample t-test resulted in 41 compounds with a p-value of less than 0.10. Of these lipids, 15 achieved p-values of less than 0.05 (**Table 3**). Of the statistically different lipids, 80% (12/15) are glycerophospholipids, suggesting that metabolism and/or regulation of these lipids is an important difference between groups. Lipid species that were identified as statistically significant were grouped according to their classes. Fold-changes were calculated between responders and non-responders (data not shown). This revealed interesting trends amongst lipid species. Relative to non-responders, responders displayed elevated levels of phosphatidylinositols, phosphatidylcholines, and alkyl/alkenyl ether phosphatidylethanolamines. In contrast, phosphatidylglycerols and phosphatidylserines were lower in responders than non-responders for both ester and ether linked fatty acid chains (**Table 5**).

Differences in Metabolite Profiles Following Treatment

Patient clinical parameters were assessed periodically over six months following rituximab therapy. Serum collected at the six month follow-up was used for metabolomics analysis. Mean 1D ^{1}H-NMR spectra at six months (**Figure 1b**) show clear differences between time points that are indicative of differential metabolic response to rituximab, as

well as, the effects of rituximab on both populations despite clinical parameters. Polar metabolite quantification from 1D ^{1}H-NMR spectra six months following rituximab therapy revealed 7 polar metabolites that attained a p-value of less than 0.10 between responders and non-responders. Five of these metabolites, succinate, taurine, lactate, pyruvate, and aspartate achieved a p-value of less than 0.05 (**Figure 2b**).

Following rituximab therapy, the composite UPLC-MS analysis of the apolar fraction of patient sera resulted in the identification of 69 lipid unique species that achieved a p-value of less than 0.10. Of these, 37 metabolites resulted in a p-value of less than 0.05 when comparing responders to non-responders (**Table 4**). Similar to the baseline data, many of these lipid species belong to the glycerophospholipid class (24/37 or 65%). Again, significant lipids were clustered into classes to identify trends. Relative fold-changes were calculated for lipid species that were significant between responders and non-responders (data not shown). Six months after treatment with rituximab, elevated levels of phosphatidic acids, phosphatidylcholines, phosphatidylserines, and alkyl/alkenyl ether phosphatidylglycerols were observed in responders relative to non-responders. Conversely, phosphatidylethanolamines, phosphatidylinositols, alkyl/alkenyl ether-phosphatidylcholines, and alkyl/alkenyl ether phosphatidylserines were lower in responders than non-responders (**Table 5**). Taken together, these trends suggest changes in glycerophospholipid metabolism that may be useful in rituximab differentiating responders from non-responders.

Multivariate Analysis of Identified Metabolites Differentiates Responders and Non-responders

Polar and apolar data sets were scaled and combined to capture the relative contribution of each metabolite to the overall differences observed between responders and non-responders. PLS-Toolbox was used to perform partial least squares discriminant analysis (PLSDA) of all identified metabolites before and after rituximab treatment. At both time points, PLSDA successfully separated responders and non-responders (**Figure 4**). PLSDA of the pre- and post-treatment metabolites shows a similar degree of separation, particularly with respect to latent variable 1 (LV1). However, separation is largely diminished in regards to latent variable 2 (LV2), reflecting the observed shifts in the metabolite profiles of both groups over time. The decrease in separation may be a signature of the metabolic shifts that are a result of the observed B cell ablation that occurs with rituximab administration independent of clinical response (8). Despite the relatively small latent variables, both PLSDA scores plots show clear separation between groups, particularly in the x-direction. The R^2 values for pre- and post-treatment analyses were 0.905234 and 0.968213, respectively.

Pathway Analysis Indicates Several Metabolic Pathway Differences Between Groups

Detected polar metabolites were mapped to known metabolic pathways using MetaboAnalyst 3.0 (36, 37). Pathways were ranked by their overall p-values. Pathways that had a statistically significant overall p-value and contained a large number of metabolite hits relative to the total number of metabolites were of particular interest. In

addition, VANTED software (38) was used to construct a metabolic pathway for the glycerophospholipids which represents the majority of the statistically significant apolar metabolites identified before and after rituximab therapy (≥65% for both). Mixed polar and apolar pathway analysis tools are not currently available, so pathway analyses were performed independently and combined to give the most comprehensive picture of the differences in metabolism between rituximab responders and non-responders (**Figure 5**). Pathway analyses were also performed at both time points to reflect metabolic changes initiated by rituximab therapy. Prior to treatment, several classes of glycerophospholipids were downregulated in responders relative to non-responders. Similarly, the polar metabolites related to these pathways were also lower in responders. Downregulation of the glycine, serine, and threonine pathway, which is connected to phosphatidylethanolamine and phosphatidylserine metabolism, is consistent with the observed relative intensities of these phospholipid classes in responders. Furthermore, choline, an essential building block for phosphatidylcholines, was reduced in responders, which is consistent with the relative downregulation of the ether linked phosphatidylcholines detected by UPLC-MS. Free glycerol was also lower in responders when compared to non-responders, which is also indicative of significant differences in glycerophospholipid metabolism between responders and non-responders prior to treatment. Taken together, these data indicate that the global metabolite signatures of responders and non-responders are distinct before treatment with rituximab.

In many cases, treatment with rituximab either ablated or reversed the trends observed before treatment. The previously detected differences in the glycine, serine, and threonine

metabolic pathway, as well as, glycerol and choline were not observed after treatment. Instead, changes in pyruvate metabolism and TCA cycle intermediates, namely lactate, pyruvate, fumarate, citrate, and succinate, contributed more significantly to differences seen between the groups following rituximab therapy. Changes in apolar metabolites involved in the glycerophospholipid pathway were consistent with their polar counterparts. Interestingly, after treatment there are unique trends between standard ester and alkyl/alkenyl ether linkage species for all major classes of phospholipids. In fact, in many cases, opposite trends were observed between linkage types for the same class of phospholipid. These differences clearly demonstrate that global metabolite signatures of responders and non-responders are distinctive following treatment with rituximab.

Global Effects of Rituximab Treatment Independent of Patient Response

When responders and non-responders were analyzed separately to compare baseline to six month follow-up, 13 polar (**Table 6**) and 23 apolar statistically significant metabolites were shared by both groups. Regardless of clinical response (responders vs. non-responders), rituximab is effective at ablating circulating B-cells (8). Common metabolic shifts between groups are therefore likely to be indicative of changes that are secondary to B-cell ablation. Pathway analysis of these metabolites were performed in MetaboAnalyst and VANTED, and manually combined. The resulting composite pathway indicates several similarities between responders (**Figure 6a**) and non-responders (**Figure 6b**). Before treatment, almost all glycerophospholipids and their related polar compounds are downregulated or not statistically significant regardless of clinical response. These include

phosphatidic acids, phosphatidylinositols, phosphatidylserines, phosphatidylcholines, choline, and phosphatidylethanolamines. Only phosphatidylglycerols were observed to be lower after rituximab treatment. Not surprisingly, more changes were observed in responders which may be a clue to understanding the observed differences in clinically relevant parameters. Overall, these data show that responders and non-responders have unique metabolic signatures before and after treatment with rituximab. In addition, rituximab therapy observably alters metabolic activity and profile signatures regardless of clinical response.

Figure 1. Mean 1D ^{1}H-NMR spectra of responders and non-responders before (a) and 6 months after (b) rituximab therapy. Variations in spectral intensities indicate unique metabolite profiles between responders and non-responders at both time points.

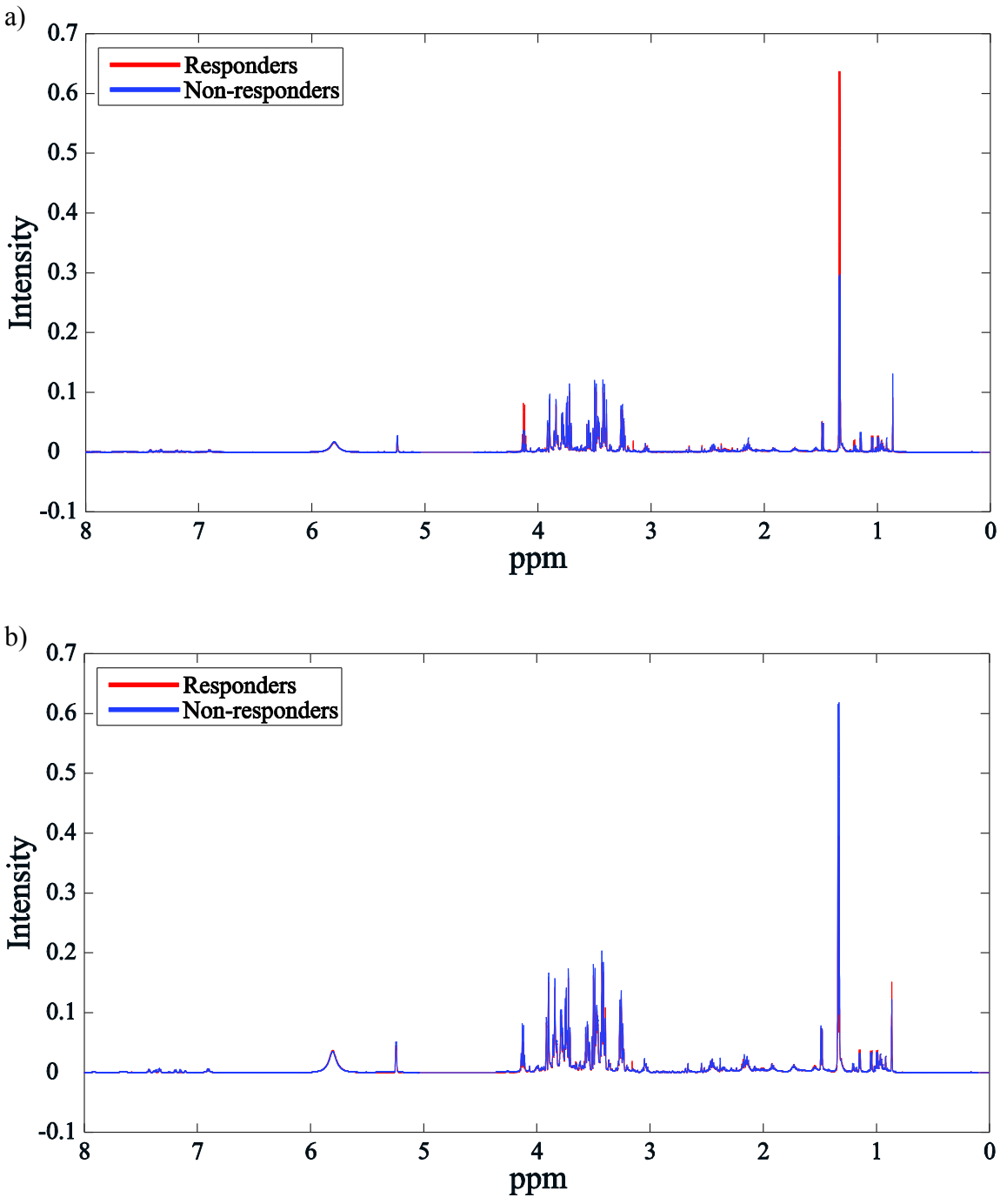

Figure 2. Significant polar metabolite concentrations in rituximab responders and non-responders. Mean concentrations (± SD) of sera polar metabolites in RA patients measured by ^{1}H-NMR before (a) and after (b) treatment with rituximab (Lactate excluded due to scale). *p<0.1 **p<0.05

a)

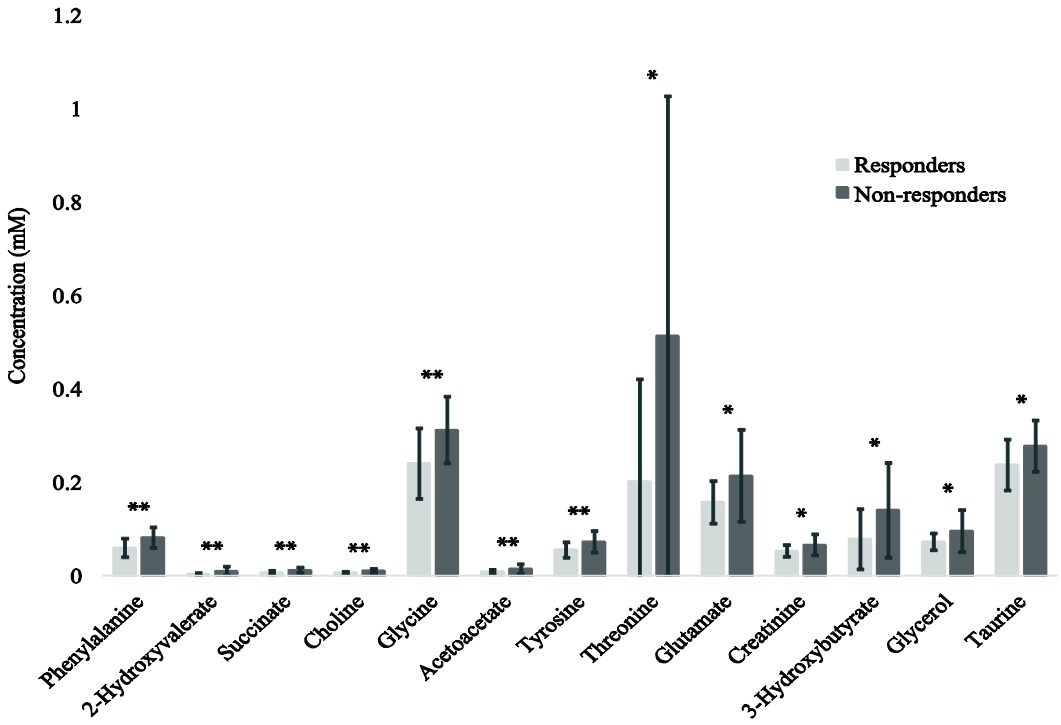

b)

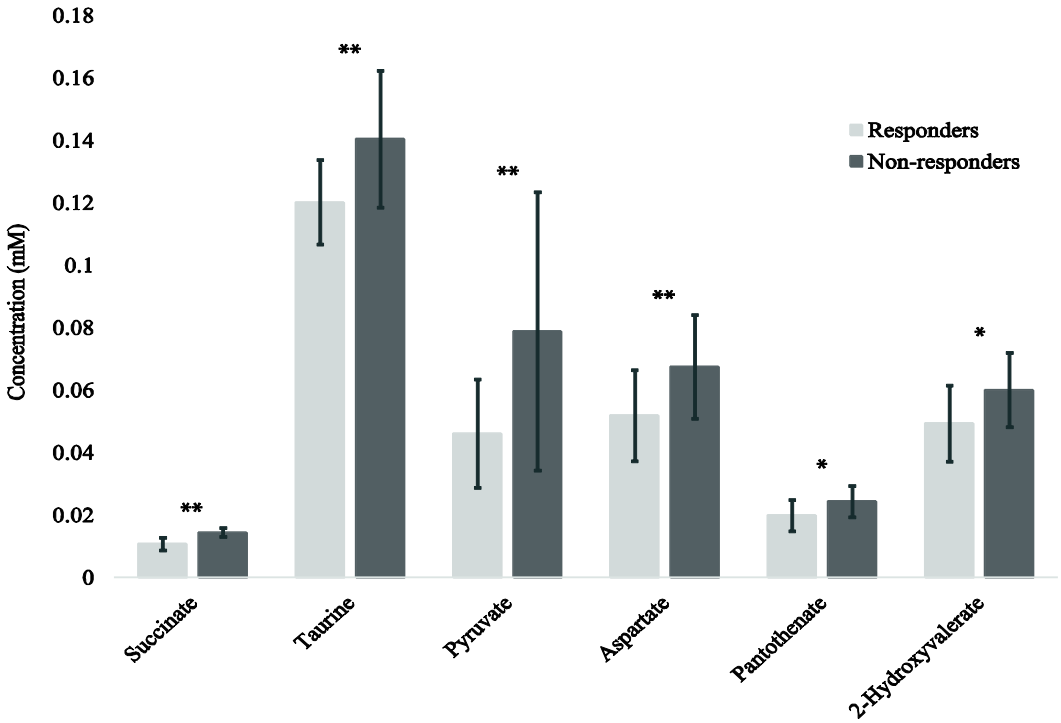

Figure 3. Heat map and hierarchical cluster analysis of polar metabolites identified by 1D ^{1}H-NMR in sera from RA patients before treatment with rituximab.

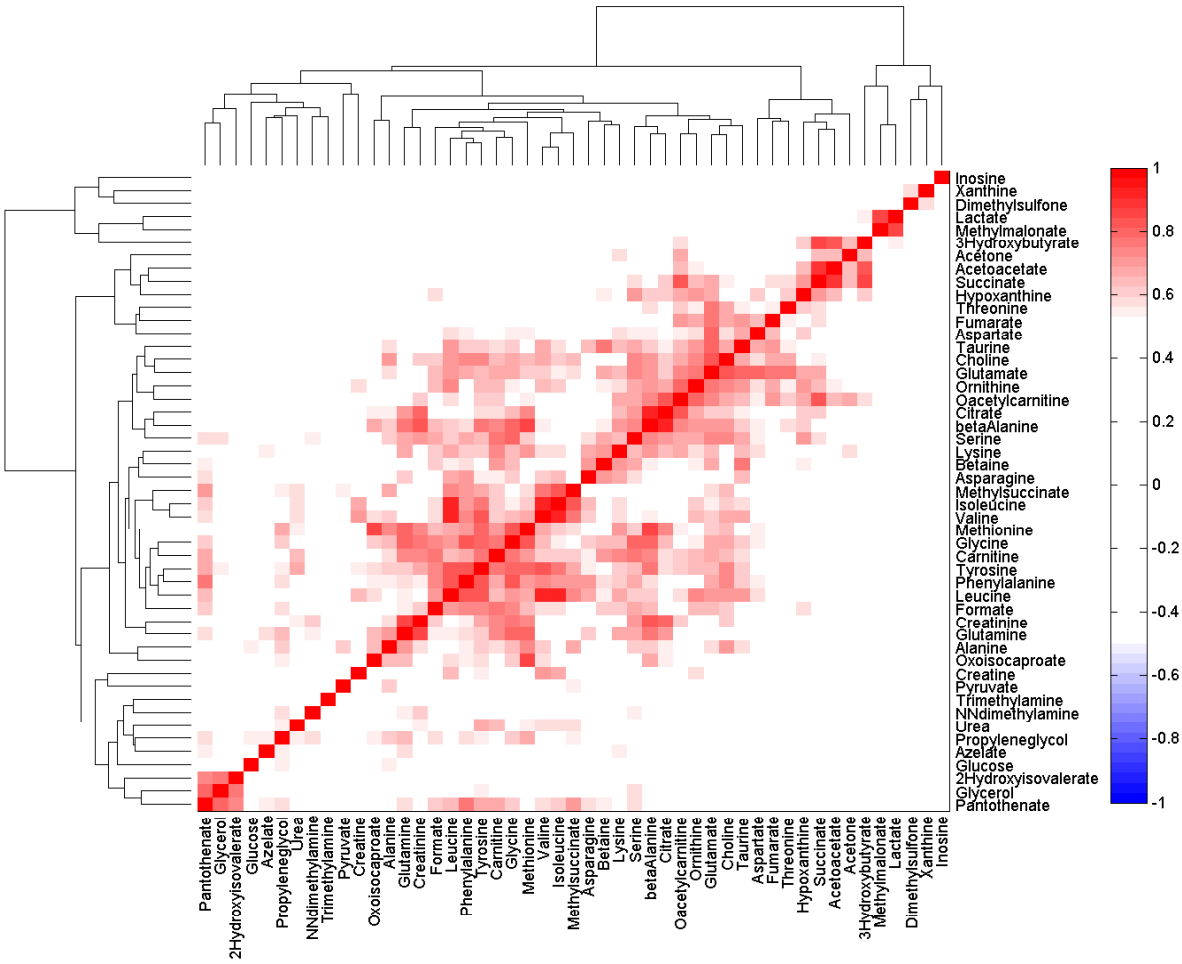

Figure 4. Partial least squares discriminant analysis of metabolites identified by 1D ^{1}H-NMR and UPLC-MS/MS in sera from rheumatoid arthritis patients. Scores plot obtained from samples collected before (a) and after (b) treatment with rituximab demonstrates group separation based on latent variables.

a)

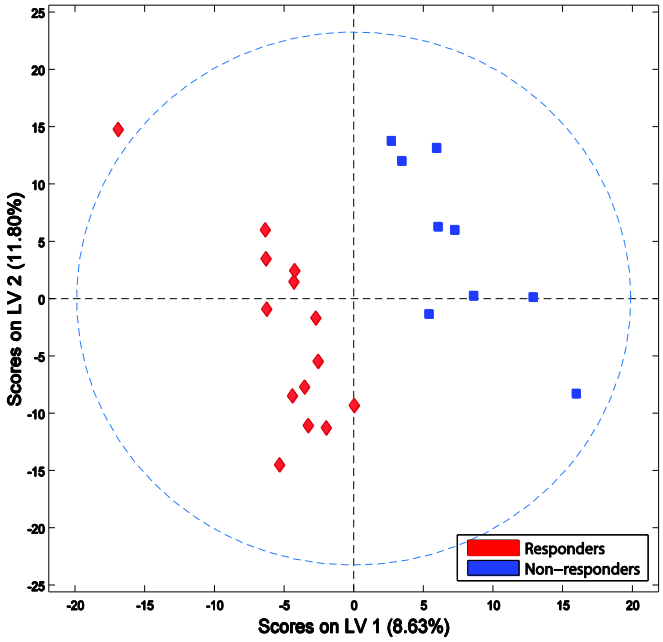

b)

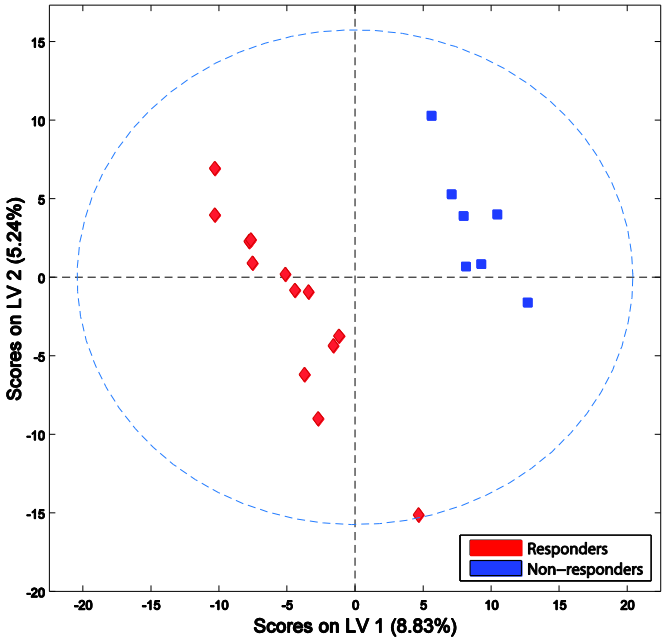

Figure 5. Pathway analysis of significant metabolite identified in RA patient sera before (a) and after (b) treatment with rituximab. Blue indicates classes that are downregulated in responders, red indicates classes that are upregulated in responders, yellow is no significant difference, and light blue indicates not detected. Split boxes represent ester linkage glycerophospholipids on the top and alkyl/alkenyl ethers on the bottom.

a)

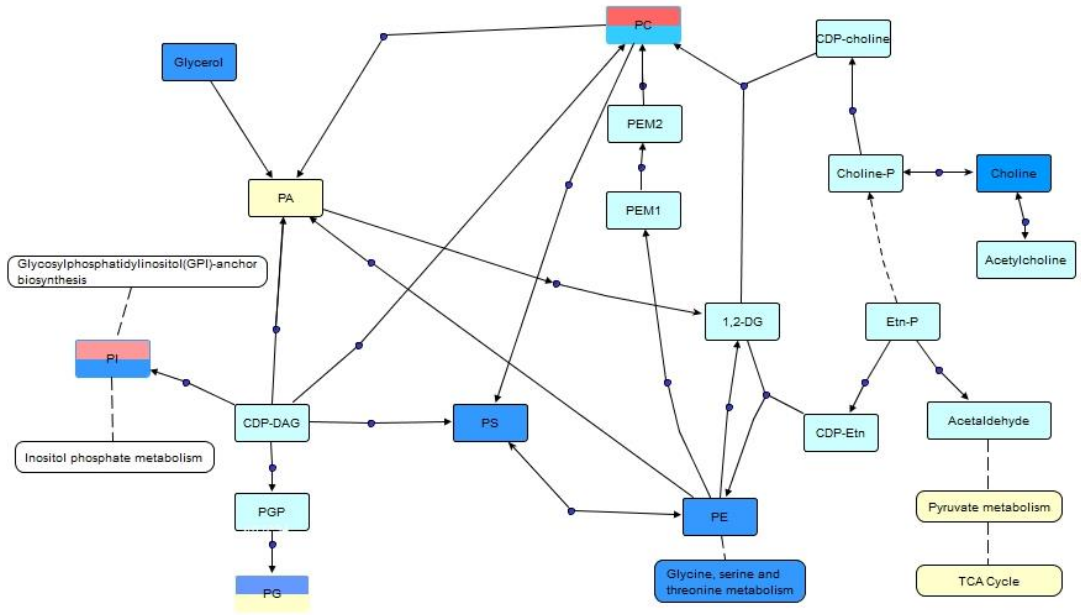

b)

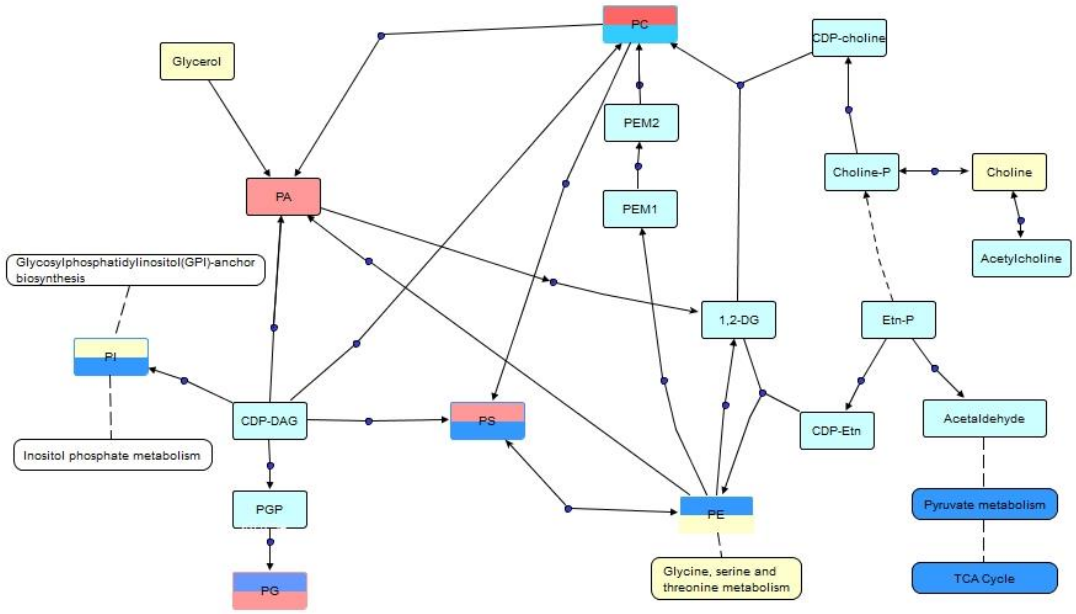

Figure 6. Pathway analysis indicating global effects of rituximab treatment in responders (a) and non-responders (b). Blue indicates classes that are downregulated after treatment, red indicates classes that are upregulated after treatment, yellow is no significant difference, and light blue indicates not detected. Split boxes represent ester linkage glycerophospholipids on the top and alkyl/alkenyl ethers on the bottom.

a)

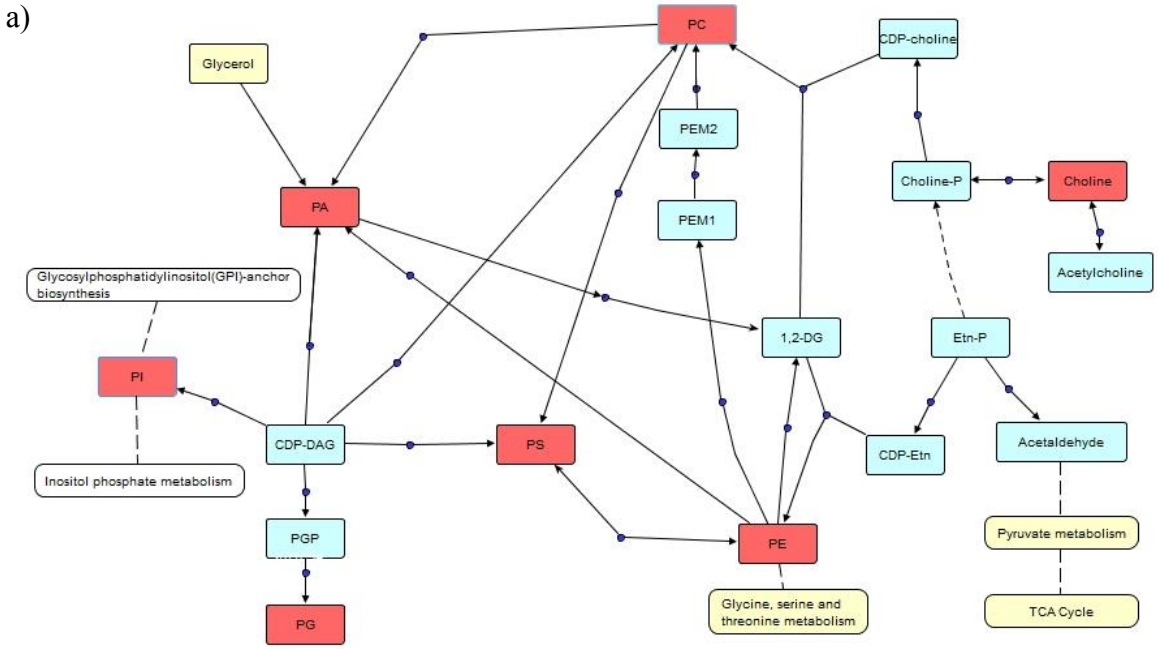

b)

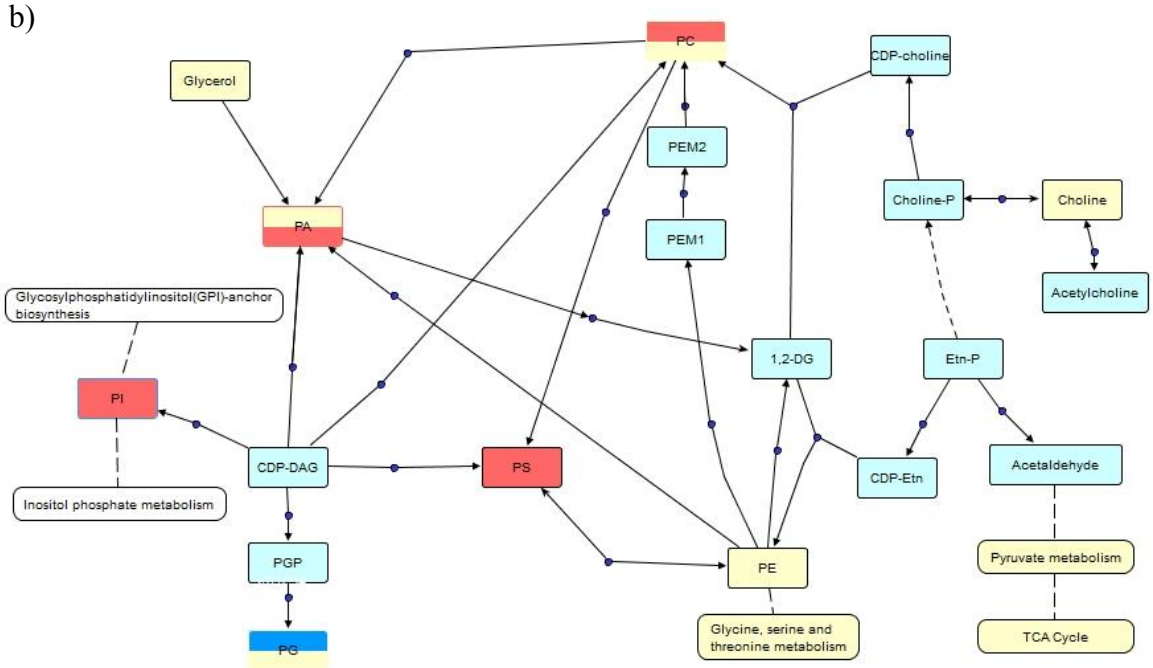

Table 1. Baseline characteristics of rheumatoid arthritis patients by response to rituximab at 6 months. MTX: Methotrexate, DAS28: 28 joint disease activity score, ESR: Erythrocyte sedimentation rate, HAQ: Health assessment questionnaire, CCP: Cyclic citrullinated peptide, ACR: American College of Rheumatology

Clinical Parameter	Responders (n = 14)	Non-responders (n = 9)
Age (years)	55.6±12.2	54.5±15.3
Female (%)	81	77
Baseline MTX Dose (mg/wk)	15.3±5.5	16.3±5.3
DAS28	6.5±0.8	6.35±1.36
ESR (mm/h)	44.2±26.4	48.8±37.2
HAQ	1.75±0.73	1.95±0.7
Pain	60.5±24.3	68.8±22.7
Swollen Joints	25.5±14.3	22.1±18.6
Tender Joints	26.8±14.1	25.5±16.7
Swollen Joints (28)	15.4±8.3	14±8.9
Tender Joints (28)	16.8±8.5	14±7.9
CCP positive (U)	188.5±252.2	76.6±56.2
ACR Response	57.2±20.9	10±15.8

Table 2. Polar metabolites identified and quantified by 1D ^{1}H-NMR before and after treatment with rituximab.
Reference values as reported in HMDB (30) were collected via NMR, unless otherwise noted. [1]GC/MS [2]HPLC [3]HPLC-Fluoroescence [4]Ion-exchange chromatography [5]DFI/MS/MS [6]Unknown. ND: No data available.

		Before				After			
		Responders		Non-Responder		Responders		Non-Responder	
Metabolite	**Normal Range (µM)**	**Mean (µM)**	**St. Dev.**	**Mean (µM)**	**St. Dev.**	**Mean (µM)**	**St. Dev.**	**Mean (µM)**	**St. Dev.**
2-Hydroxyvalerate	ND	4.74	1.92	11.15	9.49	49.41	12.20	60.12	11.87
3-Hydroxybutyrate	76.9±66.3	79.57	64.49	141.58	101.46	33.56	12.80	43.16	23.85
Acetoacetate	40.6±36.5	10.11	3.87	16.27	9.73	5.75	1.48	7.00	2.85
Acetone	54.4±29.6	15.03	7.47	18.88	12.94	16.55	6.10	16.40	4.80
Alanine	427.2±84.4	360.34	99.62	404.54	155.44	388.91	58.24	405.61	158.20
Asparagine	82.4±7.3	25.83	8.31	29.02	5.55	60.27	11.62	61.05	9.32
Aspartate	20.9±6.1	70.29	27.76	86.04	46.60	51.94	14.55	67.56	16.64
Azelate	27 (0 - 58)[1]	87.03	64.28	84.60	58.48	128.83	89.86	115.62	74.98
β-Alanine	3.8±2.9[2]	2.54	0.60	3.03	1.49	11.56	1.99	13.61	4.20
Betaine	72±22.4	52.94	16.55	63.59	18.15	50.07	10.94	54.63	10.73
Carnitine	45.7±11.6	25.50	6.58	28.05	11.30	37.92	7.60	36.32	4.19
Choline	14.5±5.3	8.07	2.42	11.62	4.93	13.70	3.20	13.40	3.45
Citrate	114.2±27	115.87	28.67	129.33	51.96	113.79	19.17	127.02	32.18
Creatine	37.6±28.3	27.25	15.73	27.14	10.47	14.77	6.58	16.75	8.85
Creatinine	86.6±18.8	54.18	12.62	67.49	22.70	58.11	9.18	65.59	11.56
Dimethylamine	48.35±7.32[2]	1.60	0.69	1.86	0.49	6.94	3.67	5.51	1.10
Dimethylsulfone	8.8±7.3	12.98	26.99	2.40	0.73	23.24	57.14	7.36	0.70
Formate	32.8±13.3	19.93	6.13	23.07	9.64	22.78	4.94	23.86	4.87
Fumarate	1.5 (0 - 4)[1]	0.88	0.45	1.33	1.25	0.40	0.57	0.54	1.00
Glucose	4971.3±372.8	4060.62	2338.39	3878.75	1549.05	4609.38	2155.66	5263.56	2549.87
Glutamate	97.4±13.2	158.66	45.85	215.36	98.52	39.60	9.98	42.85	14.07
Glutamine	510.4±118.2	513.77	136.99	535.51	156.40	376.05	57.24	396.41	97.03

Table 2, continued.

Metabolite	Normal Range (µM)	Before				After			
		Responders		Non-Responder		Responders		Non-Responder	
		Mean (µM)	St. Dev.	Mean (µM)	St. Dev.	Mean (µM)	St. Dev.	Mean (µM)	St. Dev.
Glycerol	431.6±100.4	73.64	18.02	97.32	45.11	104.56	95.48	94.08	39.17
Glycine	325.4±126.8	241.62	75.73	313.43	71.69	266.35	55.89	298.21	46.56
Hypoxanthine	34.2±10.3	13.42	5.10	21.15	21.03	11.37	4.90	13.33	4.75
Isoleucine	60.7±18.6	57.16	21.40	61.55	12.57	64.19	16.29	59.27	19.38
Lactate	1489.4±371.2	3600.75	3385.26	4101.73	2338.40	2172.43	675.38	3316.75	1387.23
Leucine	98.7±11.5	140.86	44.16	165.52	36.06	138.42	30.67	135.97	27.56
Lysine	178.6±58.2	137.43	34.31	133.63	38.50	125.45	21.36	126.06	29.17
Methionine	29.8±6.3	19.37	5.36	21.19	7.93	35.32	6.19	35.76	5.01
Methylmalonate	0.187±0.084[3]	20.07	15.16	27.40	12.46	11.67	2.90	13.38	6.14
Methylsuccinate	ND	12.70	3.24	13.73	3.59	4.17	1.15	4.03	0.67
O-acetylcarnitine	5.476±2.147[5]	3.92	1.14	4.79	1.97	3.50	0.78	4.14	0.92
Ornithine	66.9±15.3	46.38	17.91	58.77	33.95	52.20	11.01	56.31	23.86
Oxoisocaproate	28 (0 - 58)[1]	8.76	2.67	8.92	3.47	13.07	2.78	14.02	2.38
Pantothenate	4.91±0.38[6]	2.32	0.56	2.85	1.04	19.93	4.97	24.41	5.01
Phenylalanine	78.1±20.5	60.88	20.01	83.00	21.66	60.14	14.63	58.79	11.70
Propylene glycol	22.3±3.3	176.07	129.63	197.27	133.84	205.90	139.91	173.06	100.80
Pyruvate	34.5±25.2	60.52	28.81	83.40	50.28	46.13	17.31	78.89	44.55
Serine	159.8±26.6	153.98	35.48	182.14	51.03	138.51	20.37	152.02	37.89
Succinate	23.5±16.0[1]	8.01	3.83	12.88	6.11	10.82	2.02	14.46	1.44
Taurine	55±13[4]	238.77	54.21	279.25	54.72	120.23	13.56	140.44	21.89
Threonine	127.7±41	202.79	219.76	514.50	513.37	118.09	14.03	119.12	22.71
Trimethylamine	0.418±0.124[1]	0.85	0.50	1.22	0.76	1.84	0.98	2.18	1.28
Tyrosine	54.5±9.7	56.67	16.66	74.21	22.88	66.58	18.81	71.57	16.24
Urea	6074.6±2154.2	5716.72	2124.47	6101.60	2964.36	13458.43	4387.49	12896.35	4362.01
Valine	212.3±61.3	205.42	68.10	223.46	45.24	240.52	40.65	218.62	30.61
Xanthine	1.27±0.78[2]	8.01	3.01	6.06	3.56	7.08	1.83	7.22	2.69

Table 3. Lipid species identified as statistically significant between groups prior to treatment with rituximab. For simplicity, only one arrangement of each fatty acid combination is given. Alternative fatty acid combinations are indicated where appropriate. O: alkyl ether linkage, P: alkenyl ether linkage

Lipid	p-value
PS(O-20:0/18:0)/(O-16:0/22:0)	0.003566914
GlcCer(d15:1/18:0)	0.006397028
PE(O-20:0/22:6)	0.011627777
PS(22:6/20:4)	0.017446834
PC(O-17:0/20:4)	0.025489223
PC(O-16:1/2:0)/(P-16:0/2:0)/(18:1/0:0)	0.027024504
PI(P-16:0/17:2)	0.029436507
PG(17:0/21:0)/(22:0/16:0)/(19:0/19:0)/(20:0/18:0)	0.031176595
TG(17:2/17:2/18:3)/(16:1/18:3/18:3)	0.037364237
N-stearoyl glycine/N-palmitoyl GABA/Cer(d18:1/2:0)	0.03772679
PC(15:0/18:2)/(13:0/20:2)/(14:1/19:1)/(15:1/18:1)/(16:0/17:2)	0.03842968
PI(16:1/22:2)/(18:1/20:2)/(18:2/20:1)/(18:3/20:0)	0.045020992
PS(17:1/22:2)/(17:2/22:1)/(18:3/21:0)/(19:0/20:3)	0.047516211
PS(O-16:0/21:0)/(O-18:0/19:0)/(O-20:0/17:0)	0.047953259
PI(14:1/22:4)/(18:1/18:4)/(18:2/18:3)	0.049941654

Table 4. Lipid species identified as statistically significant between groups following treatment with rituximab. For simplicity, only one arrangement of each fatty acid combination is given. Alternative fatty acid combinations are indicated where appropriate. O: alkyl ether linkage, P: alkenyl ether linkage

Lipid	p-value
22:1-Glc-cholesterol/20:0-Glc-Stigmasterol/20:1-Glc-Sitosterol	0.000203202
PS(18:1/22:4)/(18:3/22:2)	0.001640816
Cer(d18:0/24:0)/(d20:0/22:0)	0.002408094
PS(O-16:0/22:4)/(O-20:0/18:4)/(O-18:0/20:4)/(P-18:0/20:3)	0.00372174
PC(15:0/18:1)/(16:0/17:1)/(13:0/20:1)/(14:0/19:1)/(14:1/19:0)/(15:0/18:1)/(15:1/18:0)	0.004483806
PS(18:0/20:4)/(18:1/20:3)/(18:2/20:2)/(18:3/20:1)	0.007527991
SM(d18:2/24:1)	0.008034291
PS(O-16:0/20:1)/(O-18:0/18:1)/(O-20:0/16:1)/(P-16:0/20:0)/(P-18:0/18:0)/(P-20:0/16:0)	0.012286441
PC(O-17:0/22:0)/PC(O-18:0/21:0)/PC(O-20:0/19:0)/PE(O-20:0/22:0)	0.013622294
PC(15:0/18:2)/(13:0/20:2)/(14:1/19:1)/(15:1/18:1)/(16:0/17:2)	0.016475796
GlcCer(d18:1/16:0)/GlcCer(d14:1/20:0)/GlcCer(d16:1/18:0)/GalCer(d18:1/16:0)	0.016499752
PG(O-20:0/22:1)(P-20:0/22:0)	0.019159837
TG(17:1/18:4/18:4)/(13:0/18:3/22:6)	0.019551953
TG(17:2/17:2/18:3)/(16:1/18:3/18:3)	0.020888891
PE(16:0/0:0)	0.02110816
PC(13:0/18:2)/(14:0/17:2)/(14:1/17:1)/(15:1/16:1)	0.023583283
PS(O-16:0/20:2)/(O-18:0/18:2)/(P-16:0/20:1)/(P-20:0/16:1)/(P-18:0/18:1)	0.023842209
PC(13:0/18:2)/(14:0/17:2)/(14:1/17:1)/(15:1/16:1)	0.024048789
SM(d18:2/22:1)	0.026786616
TG(12:0/12:0/15:1)/(12:0/13:0/14:1)	0.031351195
PC(13:0/20:4)/(15:0/18:4)/(15:1/18:3)/(15:1/18:3)	0.033131531
PS(O-16:0/22:2)/(O-18:0/20:2)/(O-20:0/18:2)/(P-16:0/22:1)/(P-18:0/20:1)	0.033432334
N-stearoyl serine	0.035653272
PC(13:0/20:4)/(15:0/18:4)/(15:1/18:3)	0.037730402
PA(O-16:0/18:3)/(P-16:0/18:2)	0.038255179
PC(O-16:0/18:1)/(O-18:0/16:1)/(O-20:0/14:1)/(P-16:0/18:0)/(P-20:0/14:0)	0.040797301
PG(O-20:0/20:0)/(O-18:0/22:0)	0.041090931
Axillarenic acid/Tetracosanedioic acid	0.041115069
beta-hydroarchaetidylglycerol	0.042645449
18:3 Campesteryl ester/ergosteryl oleate	0.042805272
PC(O-16:0/22:2)/(O-18:0/20:2)/(O-20:0/18:2)/(P-16:0/22:1)/(P-18:0/20:1)	0.044333139
PS(15:0/22:2)/(15:1/22:1)/(17:0/20:2)/(17:1/20:1)/(17:2/20:0)	0.044339139
PA(22:1/22:2)	0.045086565
Anandamide (20:2, n-6)	0.046168529
PG(21:0/22:1)	0.047224603
PC(18:0/18:1)	0.048725706
PA(12:0/21:0)/(14:0/19:0)/(17:0/16:0)/(18:0/15:0)/(20:0/13:0)	0.049716462

Table 5. Abundance of glycerophospholipid classes in responders relative to non-responders before and after treatment with rituximab. N/S: Not Significant, ↑ Upregulated in responders, ↓ Downregulated responders.

Before Treatment	Responders	After Treatment	Responders
PA	N/S	PA	↑
PC	↑	PC	↑
O/P-PC	N/S	O/P-PC	↓
PE	N/S	PE	↓
O/P-PE	↑	O/P-PE	N/S
PG	↓	PG	↓
O/P-PG	N/S	O/P-PG	↑
PI	↑	PI	N/S
O/P-PI	↓	O/P-PI	↓
PS	↓	PS	↑
O/P-PS	↓	O/P-PS	↓

Table 6. Comparison of statistically significant polar metabolites within clinical response groups. Responders and non-responders have several shared significant metabolites (shown in bold) when they are compared to themselves at baseline and 6 months. These common metabolites may be the result of effective B cell ablation by rituximab that is independent of clinical response.

Responders		Non-responders	
Metabolite	p-value	Metabolite	p-value
β-Alanine	**8.47E-15**	Dimethylsulfone	1.56E-09
2-Hydroxyvalerate	**5.13E-13**	**Pantothenate**	**4.54E-09**
Pantothenate	**9.31E-13**	**2-Hydroxyvalerate**	**2.63E-07**
Glutamate	**1.86E-09**	**Dimethylamine**	**3.64E-07**
Methylsuccinate	**2.75E-09**	**Asparagine**	**5.96E-07**
Asparagine	**3.14E-09**	**β-Alanine**	**5.56E-06**
Taurine	**5.19E-08**	**Methylsuccinate**	**6.28E-06**
Methionine	**1.62E-07**	**Taurine**	**1.98E-05**
Urea	**3.67E-06**	**Glutamate**	**0.00044**
Dimethylamine	**1.51E-05**	**Methionine**	**0.00084**
Choline	2.30E-05	**Urea**	**0.00231**
Carnitine	0.00012	**Oxoisocaproate**	**0.00508**
Oxoisocaproate	**0.00037**	Methylmalonate	0.01671
Acetoacetate	**0.00082**	Phenylalanine	0.01874
Glutamine	0.00251	**3-Hydroxybutyrate**	**0.02571**
Trimethylamine	0.00261	**Acetoacetate**	**0.02931**
Creatine	0.01375		
3-Hydroxybutyrate	**0.01837**		
Fumarate	0.02325		
Succinate	0.02662		
Aspartate	0.0436		

IV. Discussion

Despite the obvious impact of biologic agents, most studies still suggest that remission with biologic therapy is not common (40). If remission is the goal, then clearly this has not been uniformly achieved with the current biologic agents. There could be a number of reasons for this, including initiation of therapy too late in the course of disease, insufficient length of therapy, or inappropriate biological therapy. Improvement in diagnosis, treatment selection, and disease monitoring can be achieved with identification of appropriate biomarkers.

"Biomarkers are defined as anatomical, physiological, biochemical, molecular parameters or imaging features that can be used to refine diagnosis, measure the progress of diseases, or predict and monitor the effects of treatment" (11). When considering translation into clinical practice, ideal biomarkers should be minimally invasive, readily accessible, and compatible with common instrumentation. Thus, biomarkers measured in biofluids, such as blood, are preferable to those found in tissue biopsies (11, 41). Blood and urine are more suitable for RA in particular, not only because of their low invasiveness, but also because of their abundance, since early stage RA involves mostly small joints, where there is very little tissue or synovial fluid to sample (11).

Biomarkers can be separated into three major categories: diagnostic, prognostic, and predictive. Predictive biomarkers are those associated with a therapeutic response (11). These biomarkers have the potential to allow the selection of an optimal drug for a particular patient. More importantly, they may represent an essential step in patient screening that would notably allow personalized medicine models to be developed,

tailoring therapy to the individual, shortening time from onset to effective treatment, improving cost and risk-benefit ratios of drugs, and ultimately achieving high response rate with minimal toxicity. Currently, predictive biomarkers that would separate RA patient populations with respect to their outcome in response to a particular therapy is an unmet need (4, 7).

Several approaches have been tried to address this issue. So far, neither genetic, mRNA, nor protein levels in blood have successfully identified any good biomarker (42). For instance, simple measures of circulating TNF or IL-1 could not be used to predict response to TNF inhibitors (43). Furthermore, conflicting evidence has failed to provide a consistent genetic marker predictive for treatment response to TNF inhibitors. Analysis of mRNA expression is an emerging field in the identification of predictive biomarkers and, consequently, there have been few studies in this area to date. However, an analysis of TNF mRNA expression in whole-blood samples before and after treatment with infliximab found no significant difference between responders and non-responders (42). Proteomic studies to provide protein biomarkers have several advantages over studies of single candidate genes and yield more information than gained from genome or transcriptome analysis alone. Several of the proteins involved in cartilage turnover and bone resorption have been shown to be good candidates as prognostic biomarkers although many of the analyses into their potential as predictive biomarkers of response are limited by small sample sizes (44). Consequently, no robust protein biomarkers have yet been confirmed as predicting response to TNF inhibitors or other drugs.

Given the complexity and heterogeneous nature of RA, it is unlikely that a single cytokine or biomarker may provide sufficient discrimination between patients who will or will not respond to a given drug (11). Global biomarker signatures may represent more appropriate approach for improving RA patient treatment protocols and outcomes. Unlike genes and proteins, whose functions are subject to epigenetic regulation and post-translational modifications, metabolites serve as direct signatures of biochemical activity and may be easier to correlate with phenotype (45). The fundamental rationale in metabolomics is that perturbations caused by a disease in a biological system will lead to correlated changes in certain metabolite concentrations (46). Therefore, metabolite patterns and pathway changes represent the final response of biological systems to disease status or in response to a medical or external intervention (45). NMR and/or MS can delineate patterns of changes and biomarkers that are highly discriminatory for the observed disease or intervention (10). A small number of metabolomics studies have been focused on identifying metabolites associated with rheumatic diseases, primarily for diagnostic purposes (21-23), but even fewer have attempted to predict response to treatment (9).

Here we showed that both polar and apolar metabolite profiles are significantly different between RA patients who were classified as either responders or non-responders according to their ACR20 scores following treatment with rituximab. Prior to rituximab administration, 24 unique metabolites achieved p-values of less than 0.05 between patients who would later be categorized and responders and non-responders. When mapped into metabolic pathways, it becomes clear that metabolites involved in glycerophospholipid, amino acid, and energy metabolism are all important differentially regulated pathways.

Furthermore, the metabolic signatures before and after treatment were unique to each time point and treatment group. Following rituximab therapy, there were even greater differences between responders and non-responders, with 43 metabolites achieving a p-value of 0.05 or less. Interestingly, many trends between responders and non-responders were ablated and, in some cases, reversed following treatment. This is likely due to the fact that while both groups experienced loss of circulating B-cells, there is still an obvious discrepancy in metabolic response to rituximab as is indicated by clinical outcomes. Due to the indiscriminate depletion of circulating B-cells, some changes were observed in both groups following treatment. However, these similarities did not obscure or inhibit detection of additional differences that cannot be attributed to the effect of rituximab on B cells alone and therefore represent the underlying metabolic differences between responders and non-responders.

While these findings are certainly promising, more studies are needed to investigate the relationship between metabolic dysregulation and RA. In particular, there is a need for biomarkers, or more accurately, metabolic signatures for diagnosis, prognosis, and especially predictive models for enhancing therapeutic protocols. Here we evaluated a relatively small number of patients. Our findings should be validated with a large, independent group of individuals to ensure accuracy and consistency between populations. Furthermore, this study was limited in that it assessed response to a single drug. Additional studies involving anti-B cell, anti T-cell, anti-IL6, and anti-TNF biological treatments should be evaluated simultaneously to determine whether multiple therapies can be successfully distinguished prior to initiation of treatment.

V. References

1. Lawrence RC, Helmick CG, Arnett FC, Deyo RA, Felson DT, Giannini EH, Heyse SP, Hirsch R, Hochberg MC, Hunder GG, Liang MH, Pillemer SR, Steen VD, Wolfe F. 1998. Estimates of the prevalence of arthritis and selected musculoskeletal disorders in the United States. *Arthritis and Rheumatism* 41: 778-99

2. Scott DL, Wolfe F, Huizinga TWJ. 2010. Rheumatoid arthritis. *Lancet* 376: 1094-108

3. Firestein GS. 2003. Evolving concepts of rheumatoid arthritis. *Nature* 423: 356-61

4. McInnes IB, Schett G. 2011. MECHANISMS OF DISEASE The Pathogenesis of Rheumatoid Arthritis. *New England Journal of Medicine* 365: 2205-19

5. Edwards JCW, Szczepanski L, Szechinski J, Filipowicz-Sosnowska A, Emery P, Close DR, Stevens RM, Shaw T. 2004. Efficacy of B-cell-targeted therapy with rituximab in patients with rheumatoid arthritis. *New England Journal of Medicine* 350: 2572-81

6. Saag KG, Teng GG, Patkar NM, Anuntiyo J, Finney C, Curtis JR, Paulus HE, Mudano A, Pisu M, Elkins-Melton M, Outman R, Allison JJ, Almazor MS, Bridges SL, Jr., Chatham WW, Hochberg M, Maclean C, Mikuls T, Moreland LW, O'Dell J, Turkiewicz AM, Furst DE. 2008. American College of Rheumatology 2008 recommendations for the use of nonbiologic and biologic disease-modifying antirheumatic drugs in rheumatoid arthritis. *Arthritis & Rheumatism-Arthritis Care & Research* 59: 762-84

7. Cuchacovich M, Bueno D, Carvajal R, Bravo N, Carlos Aguillon J, Catalan D, Soto L. 2014. Clinical parameters and biomarkers for anti-TNF treatment prognosis in rheumatoid arthritis patients. *Clinical Rheumatology* 33: 1707-14

8. Kavanaugh A, Rosengren S, Lee SJ, Hammaker D, Firestein GS, Kalunian K, Wei N, Boyle DL. 2008. Assessment of rituximab's immunomodulatory synovial effects (ARISE trial). 1: clinical and synovial biomarker results. *Annals of the Rheumatic Diseases* 67: 402-8

9. Kapoor SR, Filer A, Fitzpatrick MA, Fisher BA, Taylor PC, Buckley CD, McInnes IB, Raza K, Young SP. 2013. Metabolic Profiling Predicts Response to Anti-Tumor

Necrosis Factor alpha Therapy in Patients With Rheumatoid Arthritis. *Arthritis and Rheumatism* 65: 1448-56

10. Priori R, Scrivo R, Brandt J, Valerio M, Casadei L, Valesini G, Manetti C. 2013. Metabolomics in rheumatic diseases: The potential of an emerging methodology for improved patient diagnosis, prognosis, and treatment efficacy. *Autoimmunity Reviews* 12: 1022-30

11. Burska A, Boissinot M, Ponchel F. 2014. Cytokines as biomarkers in rheumatoid arthritis. *Mediators of inflammation* 2014: 545493

12. Fiehn O. 2002. Metabolomics - the link between genotypes and phenotypes. *Plant Molecular Biology* 48: 155-71

13. Kim YS, Maruvada P. 2008. Frontiers in metabolomics for cancer research: Proceedings of a National Cancer Institute workshop. *Metabolomics* 4: 105-13

14. Beger RD. 2013. A review of applications of metabolomics in cancer. *Metabolites* 3: 552-74

15. Denkert C, Budczies J, Kind T, Weichert W, Tablack P, Sehouli J, Niesporek S, Koensgen D, Dietel M, Fiehn O. 2006. Mass spectrometry-based metabolic profiling reveals different metabolite patterns in invasive ovarian carcinomas and ovarian borderline tumors. *Cancer Research* 66: 10795-804

16. Kind T, Tolstikov V, Fiehn O, Weiss RH. 2007. A comprehensive urinary metabolomic approach for identifying kidney cancer. *Analytical Biochemistry* 363: 185-95

17. Pirman DA, Efuet E, Ding X-P, Pan Y, Tan L, Fischer SM, DuBois RN, Yang P. 2013. Changes in Cancer Cell Metabolism Revealed by Direct Sample Analysis with MALDI Mass Spectrometry. *Plos One* 8

18. Sugimoto M, Wong DT, Hirayama A, Soga T, Tomita M. 2010. Capillary electrophoresis mass spectrometry-based saliva metabolomics identified oral, breast and pancreatic cancer-specific profiles. *Metabolomics* 6: 78-95

19. Tiziani S, Lopes V, Gunther UL. 2009. Early Stage Diagnosis of Oral Cancer Using H-1 NMR-Based Metabolomics. *Neoplasia* 11: 269-U69

20. Tiziani S, Kang Y, Harjanto R, Axelrod J, Piermarocchi C, Roberts W, Paternostro G. 2013. Metabolomics of the Tumor Microenvironment in Pediatric Acute Lymphoblastic Leukemia. *Plos One* 8

21. Madsen RK, Lundstedt T, Gabrielsson J, Sennbro C-J, Alenius G-M, Moritz T, Rantapaa-Dahlqvist S, Trygg J. 2011. Diagnostic properties of metabolic perturbations in rheumatoid arthritis. *Arthritis Research & Therapy* 13

22. Kim S, Hwang J, Xuan J, Jung YH, Cha H-S, Kim KH. 2014. Global Metabolite Profiling of Synovial Fluid for the Specific Diagnosis of Rheumatoid Arthritis from Other Inflammatory Arthritis. *Plos One* 9

23. Kosinska MK, Liebisch G, Lochnit G, Wilhelm J, Klein H, Kaesser U, Lasczkowski G, Rickert M, Schmitz G, Steinmeyer J. 2013. A Lipidomic Study of Phospholipid Classes and Species in Human Synovial Fluid. *Arthritis and Rheumatism* 65: 2323-33

24. Prevoo MLL, Vanthof MA, Kuper HH, Vanleeuwen MA, Vandeputte LBA, Vanriel P. 1995. MODIFIED DISEASE-ACTIVITY SCORES THAT INCLUDE 28-JOINT COUNTS - DEVELOPMENT AND VALIDATION IN A PROSPECTIVE LONGITUDINAL-STUDY OF PATIENTS WITH RHEUMATOID-ARTHRITIS. *Arthritis and Rheumatism* 38: 44-8

25. Tiziani S, Einwas A-H, Lodi A, Ludwig C, Bunce CM, Viant MR, Guenther UL. 2008. Optimized metabolite extraction from blood serum for H-1 nuclear magnetic resonance spectroscopy. *Analytical Biochemistry* 377: 16-23

26. Hwang TL, Shaka AJ. 1995. WATER SUPPRESSION THAT WORKS - EXCITATION SCULPTING USING ARBITRARY WAVE-FORMS AND PULSED-FIELD GRADIENTS. *Journal of Magnetic Resonance Series A* 112: 275-9

27. Ludwig C, Guenther UL. 2011. MetaboLab - advanced NMR data processing and analysis for metabolomics. *Bmc Bioinformatics* 12

28. Parsons HM, Ludwig C, Guenther UL, Viant MR. 2007. Improved classification accuracy in 1-and 2-dimensional NMR metabolomics data using the variance stabilising generalised logarithm transformation. *Bmc Bioinformatics* 8

29. Ludwig C, Easton JM, Lodi A, Tiziani S, Manzoor SE, Southam AD, Byrne JJ, Bishop LM, He S, Arvanitis TN, Guenther UL, Viant MR. 2012. Birmingham Metabolite Library: a publicly accessible database of 1-D H-1 and 2-D H-1 J-resolved NMR spectra of authentic metabolite standards (BML-NMR). *Metabolomics* 8: 8-18

30. Wishart DS, Tzur D, Knox C, Eisner R, Guo AC, Young N, Cheng D, Jewell K, Arndt D, Sawhney S, Fung C, Nikolai L, Lewis M, Coutouly MA, Forsythe I, Tang P, Shrivastava S, Jeroncic K, Stothard P, Amegbey G, Block D, Hau DD, Wagner J, Miniaci J, Clements M, Gebremedhin M, Guo N, Zhang Y, Duggan GE, Macinnis GD, Weljie AM, Dowlatabadi R, Bamforth F, Clive D, Greiner R, Li L, Marrie T, Sykes BD, Vogel HJ, Querengesser L. 2007. HMDB: the Human Metabolome Database. *Nucleic Acids Res* 35: D521-6

31. Kanehisa M, Goto S, Sato Y, Kawashima M, Furumichi M, Tanabe M. 2014. Data, information, knowledge and principle: back to metabolism in KEGG. *Nucleic Acids Research* 42: D199-D205

32. Fahy E, Subramaniam S, Murphy RC, Nishijima M, Raetz CRH, Shimizu T, Spener F, van Meer G, Wakelam MJO, Dennis EA. 2009. Update of the LIPID MAPS comprehensive classification system for lipids. *Journal of Lipid Research* 50: S9-S14

33. Cui Q, Lewis IA, Hegeman AD, Anderson ME, Li J, Schulte CF, Westler WM, Eghbalnia HR, Sussman MR, Markley JL. 2008. Metabolite identification via the Madison Metabolomics Consortium Database. *Nature Biotechnology* 26: 162-4

34. Smith CA, O'Maille G, Want EJ, Qin C, Trauger SA, Brandon TR, Custodio DE, Abagyan R, Siuzdak G. 2005. METLIN - A metabolite mass spectral database. *Therapeutic Drug Monitoring* 27: 747-51

35. Zhou B, Wang J, Ressom HW. 2012. MetaboSearch: Tool for Mass-Based Metabolite Identification Using Multiple Databases. *Plos One* 7

36. Xia J, Mandal R, Sinelnikov IV, Broadhurst D, Wishart DS. 2012. MetaboAnalyst 2.0-a comprehensive server for metabolomic data analysis. *Nucleic Acids Research* 40: W127-W33

37. Xia J, Psychogios N, Young N, Wishart DS. 2009. MetaboAnalyst: a web server for metabolomic data analysis and interpretation. *Nucleic Acids Research* 37: W652-W60

38. Klukas C, Schreiber F. 2010. Integration of -omics data and networks for biomedical research with VANTED. *Journal of integrative bioinformatics* 7: 112-

39. Goeman JJ, van de Geer SA, de Kort F, van Houwelingen HC. 2004. A global test for groups of genes: testing association with a clinical outcome. *Bioinformatics* 20: 93-9

40. Saleem B, Keen H, Goeb V, Parmar R, Nizam S, Hensor EMA, Churchman SM, Quinn M, Wakefield R, Conaghan PG, Ponchel F, Emery P. 2010. Patients with RA in remission on TNF blockers: when and in whom can TNF blocker therapy be stopped? *Annals of the Rheumatic Diseases* 69: 1636-42

41. Rifai N, Gillette MA, Carr SA. 2006. Protein biomarker discovery and validation: the long and uncertain path to clinical utility. *Nature Biotechnology* 24: 971-83

42. Emery P, Doerner T. 2011. Optimising treatment in rheumatoid arthritis: a review of potential biological markers of response. *Annals of the Rheumatic Diseases* 70: 2063-70

43. Charles P, Elliott MJ, Davis D, Potter A, Kalden JR, Antoni C, Breedveld FC, Smolen JS, Eberl G, deWoody K, Feldmann M, Maini RN. 1999. Regulation of cytokines, cytokine inhibitors, and acute-phase proteins following anti-TNF-alpha therapy in rheumatoid arthritis. *Journal of Immunology* 163: 1521-8

44. Hueber W, Tomooka BH, Batliwalla F, Li WT, Monach PA, Tibshirani RJ, Van Vollenhoven RF, Lampa J, Saito K, Tanaka Y, Genovese MC, Klareskog L, Gregersen PK, Robinson WH. 2009. Blood autoantibody and cytokine profiles predict response to anti-tumor necrosis factor therapy in rheumatoid arthritis. *Arthritis Research & Therapy* 11: 13

45. Semerano L, Romeo P-H, Boissier M-C. 2015. Metabolomics for rheumatic diseases: has the time come? *Annals of the Rheumatic Diseases* 74: 1325-6

46. Patti GJ, Yanes O, Siuzdak G. 2012. Metabolomics: the apogee of the omics trilogy. *Nature Reviews Molecular Cell Biology* 13: 263-9